Optik 140 (2017) 1032–1037

Contents lists available at ScienceDirect

Optik

journal homepage: www.elsevier.de/ijleo

Original research article

Characterization of MWCNT-TiO_2 QDs and TiO_2 QDs in self-assembled films

Ümit Özlem Akkaya Arıer[a,*], Bengü Özuğur Uysal[b]

[a] Department of Physics, Mimar Sinan Fine Arts University, Bomonti, Istanbul 34349, Turkey
[b] Faculty of Engineering and Natural Sciences, Kadir Has University, Cibali Campus, Fatih, Istanbul 34083, Turkey

ARTICLE INFO

Article history:
Received 22 November 2016
Received in revised form 26 April 2017
Accepted 28 April 2017

Keywords:
MWCNT-TiO_2
QDs composites
Films
Growth kinetics

ABSTRACT

In this study, the solution which includes TiO_2 quantum dots (QDs) was mixed with the multi-wall carbon nanotubes (MWCNTs) to prepare MWCNT-TiO_2 QDs composite films. The effect of microstructures on the structural and optical properties of MWCNT-TiO_2 QDs composite films was evaluated. The activation energy for crystallite growth of TiO_2 QDs which are produced in brookite phases was calculated as 20.3 kJ/mol. The properties of MWCNT-TiO_2 QDs composite films were characterized by X-ray diffraction (XRD), scanning electron microscopy (SEM), atomic force microscopy (AFM) and ultraviolet–visible absorption spectroscopy (UV–vis).

1. Introduction

Single-walled and multi-walled carbon nanotubes (CNTs) have interesting physical and technological properties. CNTs have large surface areas, high strength and good electrical conductivities [1,3]. MWCNT-TiO_2 composite structures have a number of applications including photocatalytic and hydrophilic activities, solar cells, lithium ion batteries, biosensors and electrochemical capacitor due to their mechanical, chemical and electrical properties [2–12]. MWCNT-TiO_2 composites show higher photocatalytic activity than pure TiO_2 structures [2,13]. MWCNT-TiO_2 structures have been prepared with different methods such as sol-gel deposition, chemical vapor deposition (CVD), hydrothermal deposition, and electrospinning deposition etc. [1–3,13]. MWCNT-TiO_2 QDs composites can be produced as powder, films, etc. [4–6]. Combining TiO_2 films with CNTs improves aspects such as mechanical and optoelectronic efficiency [14]. TiO_2 quantum dots have different properties because of quantum confinement effects, small size, and high surface area. If the particle size is comparable to the Bohr exciton radius of the material, one can investigate that this material which contain QDs display quantum confinement effects considerably. Only if radius of particles is smaller than exciton radius, particles exhibit strong confinement. While exciton Bohr radius of hydrogen: 0.53 Å, the exciton radii of TiO_2 nano-particles are between 7.5 and 19 Å [15]. Quantum size effect occurred in TiO_2 particles which have radius in the range of 1–10 nm [16,17]. Quantum size effect of QDs means controlling the band gap, thus tuning the discreteness of the energy levels depending on the size. Brookite phase of TiO_2 is difficult to produce purely and there is no any study about brookite phase of MWCNT-TiO_2 QDs composite films [16]. The effect of precursor ratios on the film is here presented where TiO_2 quantum dots are incorporated in the film structure in addition with MWCNT in order to form the dispersed media of TiO_2 QDs in MWCNT-TiO_2 films.

* Corresponding author.
E-mail address: oarier@gmail.com (Ü.Ö.A. Arıer).

http://dx.doi.org/10.1016/j.ijleo.2017.04.101
0030-4026/

Table 1
Size calculations of QDs from XRD and UV–vis measurements by using Scherrer and Brus equations for different Acid:TiO_2 ratios.

Data	Acid:TiO_2 ratio	Xrd graph Scherrer's equ. QD size (nm)	Brus equ. QDs size (nm)
a	0.05	2.99	2.18
b	0.1	3.58	3.81
c	0.2	4.22	4.13
d	0.4	5.52	5.15

2. Experimental

2.1. Preparation of solutions and coatings

TiO_2 QDs and MWCNT-TiO_2 QDs composite thin films were prepared using sol-gel method. TiO_2 solution was prepared by dissolving 1.2 ml titanium isopropoxide $Ti(OCH(CH_3)_2)_4$ in the solution which contains 11 ml ethanol, 0.12 ml acetic acid (AcAc) and 0.038 ml water. Firstly, titanium isopropoxide, ethanol and water concentrations were held fixed, and then acid:TiO_2 volume ratios were changed to 0.4, 0.2, 0.1, 0.05.

Secondly, TiO_2 solution (acid:TiO_2 volume ratios: 0.05) and MWCNT (outer diameter 20–40 nm, cheaptubes-commercial) were used to prepare the four different solutions for MWCNT:TiO_2 ratio: 0.005, 0.00375, 0.0025 and 0.00125. The solutions were mixed using a magnetic stirrer for 3 h and then they were deposited on corning 2947 glass substrates by a spin-coating technique with a speed of 3000 rpm. Eight different sol-coated glass substrates were annealed at 470 °C. The process was repeated at 420, 520, and 570 °C heat treatment temperatures for TiO_2 QDs contained film with volume ratio of acid:TiO_2 = 0.2.

2.2. Characterization of coatings

TiO_2 QDs and MWCNT-TiO_2 QDs composite films deposited on glass substrates were characterized by X-ray diffractometer (XRD, Philips PW-1800, Cu-Kα radiation). A scanning electron microscopy (SEM-S-3100H, Hitachi Ltd.) and atomic force microscope (AFM, Shimadzu scanning probe microscope SPM-9500J3) were used to investigate the surface morphology of these films. UV–vis spectroscopic analysis of films was performed using UV–visible absorption spectrophotometer (Perkin–Elmer Lambda 900 with Labsphere integrating software).

3. Results and discussion

3.1. XRD analysis

XRD was employed to study the crystal structure of the prepared films. TiO_2 QDs films which were produced with various acid:TiO_2 ratios and MWCNT-TiO_2 QDs composite films for different MWCNT:TiO_2 ratios were analyzed in Fig. 1.

The diffraction patterns of the films demonstrate that both TiO_2 QDs and MWCNT-TiO_2 QDs films included brookite (orthorhombic) phase of (211) (JCPDS card No. 75-1582) [17].

The crystal sizes of TiO_2 QDs for different acid:TiO_2 ratios and TiO_2 QDs in MWCNT-TiO_2 QDs composite film are calculated with Scherrer's formula according to the XRD results. They are displayed in Table 1. TiO_2 QDs crystal sizes were determined between 2.99 and 5.52 nm for different acid:TiO_2 ratios and these values were found near the TiO_2 exciton Bohr radius. The results indicate that a decrease in the ratio leads to the increase in the TiO_2 QDs size. That is to say, the sizes of TiO_2 QDs decreased with the increase in acid:TiO_2 ratios due to the accelerated reaction with the increase in the amount of acid. Furthermore, the increase in the amount of TiO_2 causes the agglomeration, so the crystal size of TiO_2 QDs in MWCNT-TiO_2 QDs composite films increases with this increment.

The activation energy of TiO_2 QDs films was calculated by Arrhenius equation. The average QDs size (d) can be determined using Eq. (1): a is the intercept, R is the universal gas constant, T is the temperature (Kelvin), and E is the activation energy.

$$\ln d = -E/RT + \ln a \quad (1)$$

Fig. 2 represents a plot of logarithm of the particle size versus the temperature (1000/T). The activation energy for the TiO_2 QDs growth was determined using the slope of the line in Fig. 2 and Eq. (1) as 20.3 kJ/mol. The activation energy of the rare brookite phase has been found less than the values of other phases in the literature because of the difficulties in obtaining brookite crystal phase. In this case, the total surface energy increases and that leads to growth of QDs require less energy.

TEM images of TiO_2 QDs are shown in Fig. 3. The particles size was approximately determined as 5 nm for acid:TiO_2 ratio of 0.05. TEM images of the films are difficult to measure because the films are very thin.

SEM and AFM images of TiO_2 QDs and MWCNT-TiO_2 QDs composite films are shown in Fig. 4 and Fig. 5. Fig. 4 indicate that TiO_2 QDs were located on the MWCNTs. Surface roughness values of the films were determined to be Rms: 5.07; 5.65; 6.80; 8.22 nm for MWCNT:TiO_2 ratios of 0.005, 0.00375, 0.0025 and 0.00125, respectively. For different acid:TiO_2 ratios of

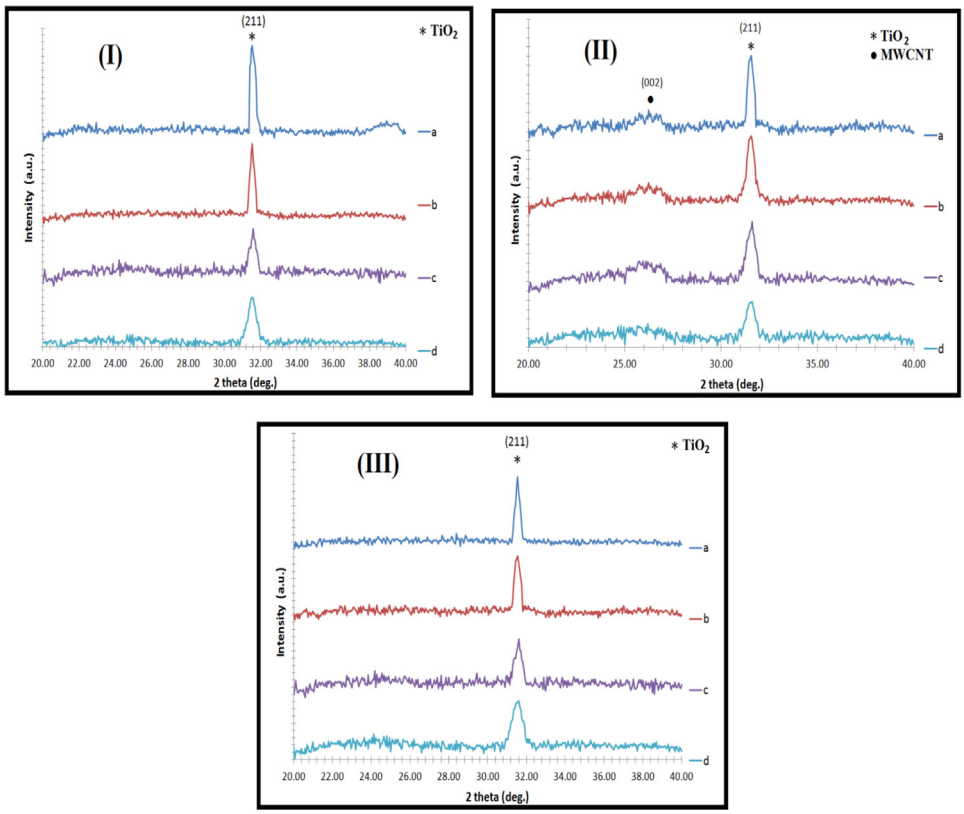

Fig. 1. X-ray diffraction patterns of (I) TiO_2 QDs films for different acid:TiO_2 ratios: (a) 0.05, (b) 0.1, (c) 0.2, (d) 0.4; (II) MWCNT-TiO_2 QDs composites films for different MWCNT:TiO_2 ratios: (a) 0.00125, (b) 0.0025, (c) 0.00375, (d) 0.005, (III) TiO_2 QDs films for different heat treatment temperatures: (a) 570, (b) 520, (c) 470, (d) 420 °C for acid:TiO_2 volume ratios: 0.05.

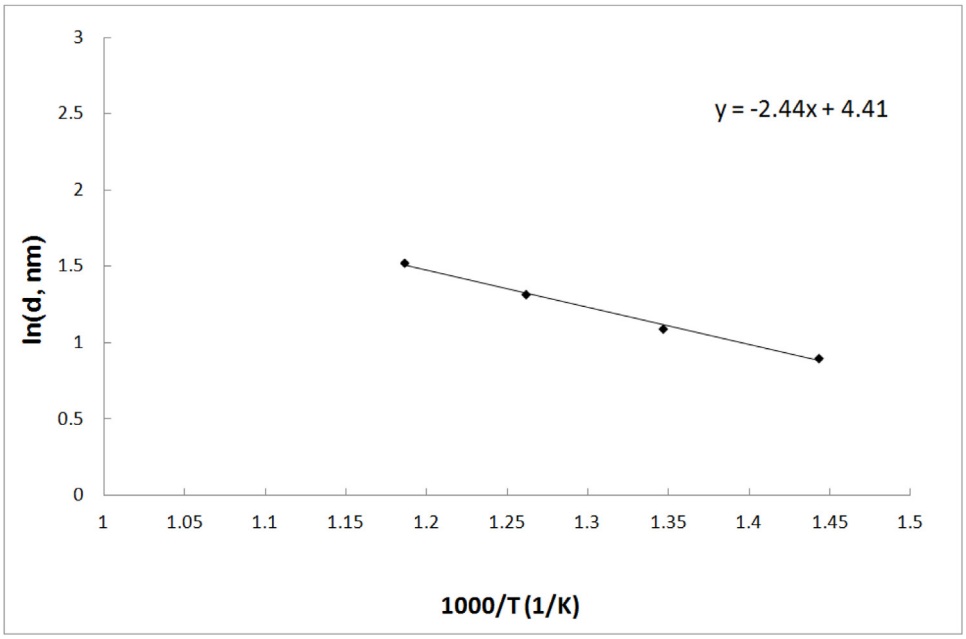

Fig. 2. Arrhenius plot of TiO_2 QDs films for acid:TiO_2 volume ratios: 0.05.

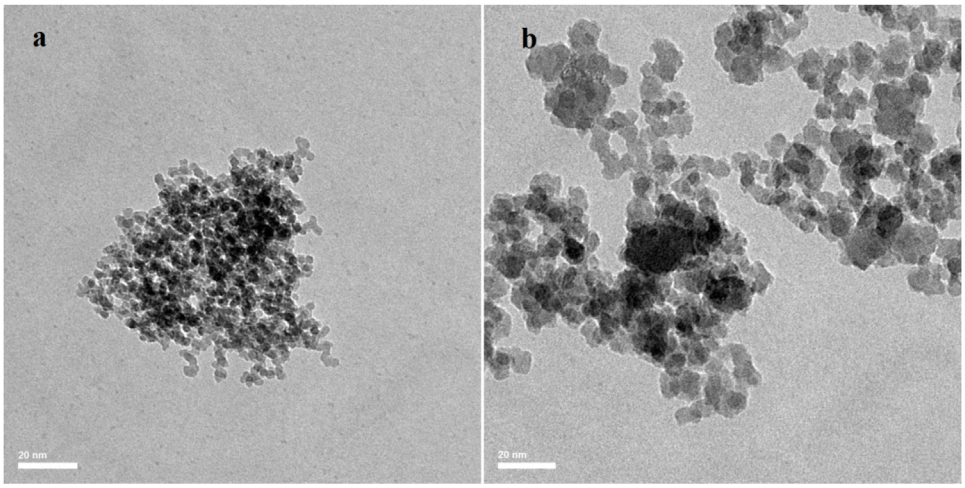

Fig. 3. TEM images of TiO_2 QDs with different acid:TiO_2 ratios: (a) 0.1, (b) 0.05.

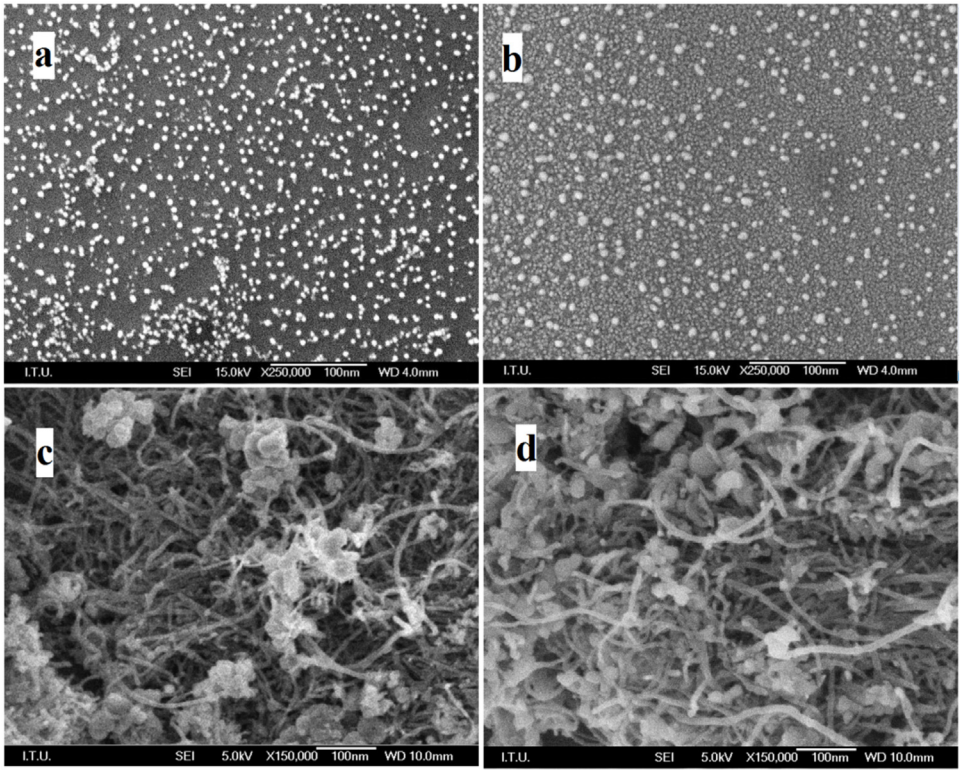

Fig. 4. SEM images of TiO_2 with different acid:TiO_2 ratios: (a) 0.1, (b) 0.05, MWCNT-TiO_2 QDs composite films with different MWCNT:TiO_2 ratios: (c) 0.005, (d) 0.0025.

to 0.4, 0.2, 0.1, 0.05, the roughness values were evaluated to be Rms: 1.9; 2.2; 3.5; 4.51. The roughness increased with the decreasing acid:TiO_2 and MWCNT:TiO_2 ratios.

Absorption graphs of TiO_2 QDs and MWCNT-TiO_2 QDs composite films are represented in Fig. 6. When MWCNT's amount was held fixed, absorption edge shifts to a longer wavelength by increasing the TiO_2 ratios.

The sizes of TiO_2 QDs can be calculated using the absorption shift and effective mass model (particle in a box problem) by Brus equation in Fig. 6 [18]. QDs' sizes were determined from the relationship between band gap shift (ΔEg) and radius

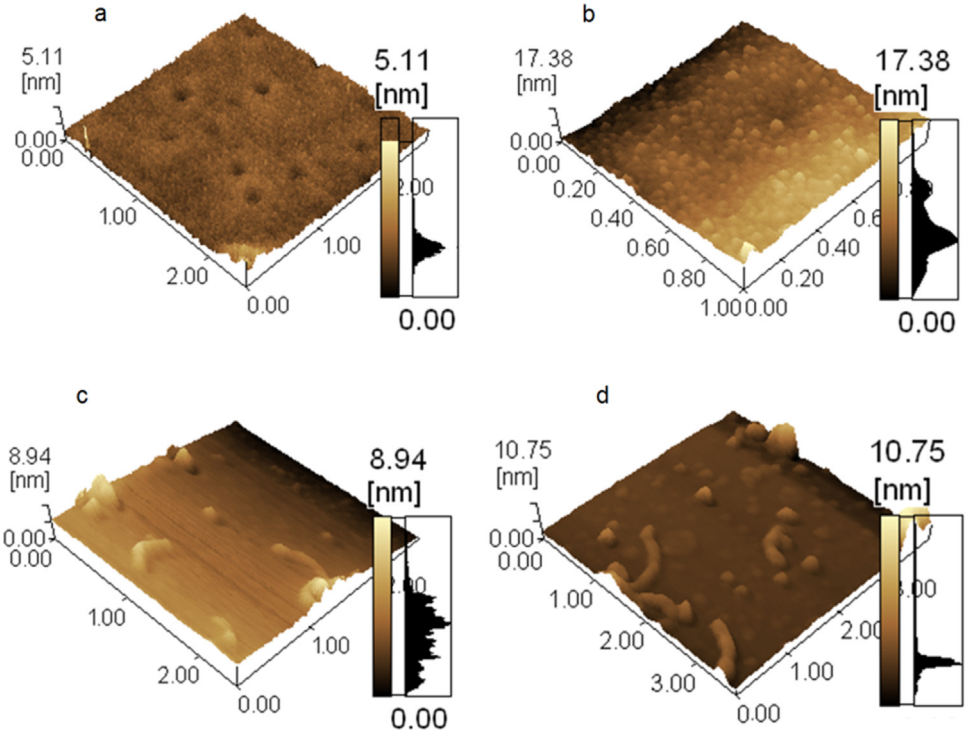

Fig. 5. AFM images of TiO_2 with different acid:TiO_2 ratios: (a) 0.1, (b) 0.05, MWCNT-TiO_2 QDs composite films with different MWCNT:TiO_2 ratios: (c) 0.005, (d) 0.0025.

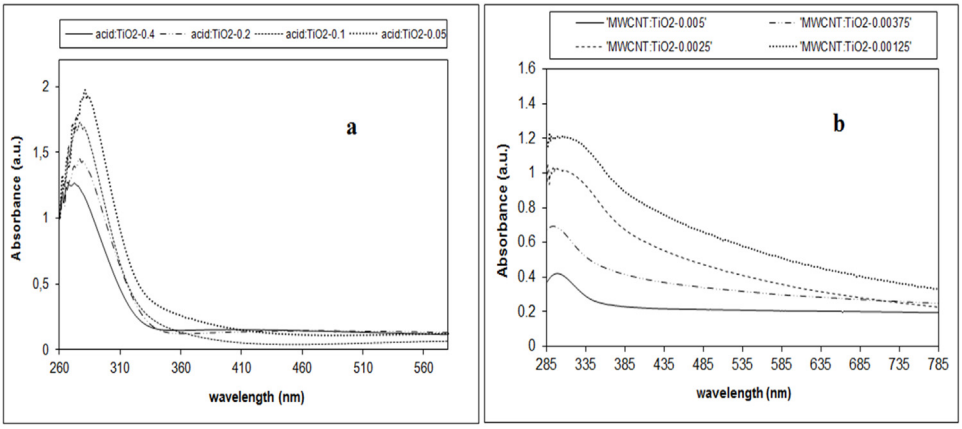

Fig. 6. UV–vis spectra of (a) TiO_2 QDs films for different acid:TiO_2 ratios: 0.4; 0.2; 0.1; 0.05, (b) MWCNT-TiO_2 QDs composite films for different MWCNT:TiO_2 ratios: 0.005; 0.00375; 0.0025; 0.00125.

(r) of QDs using Eq. (2), where h is Planck's constant, μ effective mass, ε is the dielectric constant, $\Delta Eg = E_g - E_{bulk}$ is the band gap shift. Effective mass for TiO_2 is taken as 1.63mo, which is experimentally estimated by Kormann et al. [19,20].

$$E_{\min} = E_g + \frac{h---^2\pi^2}{2\mu r^2} - \frac{1.8e^2}{4\pi\epsilon_0\epsilon r} \tag{2}$$

If radius of QDs is smaller than exciton radius, the first term is dominant as quantum confinement in the equation, and the last term is because of the Coulomb interaction between the electron and the hole in Eq. (1).

Xrd and uv results of TiO_2 QDs' sizes were compared, and it was found that the sizes increased with acid:TiO_2 ratios in Table 1. The UV–vis absorption spectra represent that absorption edge shifts to a longer wavelength with the increasing QDs' sizes.

4. Conclusions

TiO_2 QDs and MWCNT-TiO_2 QDs composite films were deposited by sol-gel spin coating technique. QDs sizes of the films depend on the precursor ratios such as acid:TiO_2 and MWCNT:TiO_2 ratios. TiO_2 QDs and MWCNT-TiO_2 QDs composite films were obtained as brookite form and single oriented (211). TiO_2 QDs dispersed easily in MWCNT-TiO_2 QDs composite films. It is found that size of TiO_2 QDs can be controlled by changing the acid:TiO_2 and MWCNT:TiO_2 ratios. The sizes of particles were determined with different ways in Table 1. The films exhibit absorption in the longer wavelength region with the increment QDs size. With the optimization of the process parameters, untoxic TiO_2 films including QDs in preferred sizes and features can be used in optic and electronic industry.

Acknowledgment

The Research Fund of Mimar Sinan Fine Arts University (BAP Project No: 201206) has supported this research.

References

[1] S. Wang, L.J. Ji, B. Wu, Q. Gong, Y. Zhu, J. Liang, Influence of surface treatment on preparing nanosized TiO2 supported on carbon nanotubes, Appl. Surf. Sci. 255 (2008) 3263–3266.
[2] H. Yu, X. Quan, S. Chen, H. Zhao, Y. Zhang, TiO_2–carbon nanotube heterojunction arrays with a controllable thickness of TiO2 layer and their first application in photocatalysis, J. Photochem. Photobiol. A: Chem. 200 (2008) 301–306.
[3] H. Kim, H.J. Kim, M. Morita, S.G. Park, Preparation and electrochemical performance of CNT electrode with deposited titanium dioxide for electrochemical capacitor, Bull. Korean Chem. Soc. 31 (2010) 423–428.
[4] K. Woan, G. Pyrgiotakis, W. Sigmund, Photocatalytic Carbon-Nanotube–TiO_2 composites, Adv. Mater. 21 (2009) 2233–2239.
[5] M.J. Sampaio, C.G. Silva, R.R.N. Marques, A.M.T. Silva, J.L. Faria, Carbon nanotube–TiO2 thin films for photocatalytic applications, Catal. Today 161 (2011) 91–96.
[6] W. Jarernboon, S. Pimanpang, S. Maensiri, E. Swatsitang, V. Amornkitbamrung, Effects of multiwall carbon nanotubes in reducing microcrack formation on electrophoretically deposited TiO, J. Alloys Compd. 476 (2009) 840–846.
[7] W.Q. Zhang, G.B. Zhu, J.Y. Ma, X.H. Zhang, J.H. Chen, A new electrochemical sensor based on W-doped titania-CNTs composite for detection of pentachlorophenol, Indian J. Chem. 50 (2011) 15–21.
[8] Y. Tang, L. Liu, X. Wang, D. Jia, W. Xia, Z. Zhao, J. Qiu, TiO_2 quantum dots embedded in bamboo-like porous carbon nanotubes as ultra high power and long life anodes for lithium ion batteries, J. Power Sources 319 (2016) 227–234.
[9] K.R. Reddy, M. Hassan, V.G. Gomes, Hybrid nanostructures based on titanium dioxide for enhanced photocatalysis, Appl. Cat. A: Gen. 489 (2015) 1–16.
[10] Z. Peining, A.S. Nair, Y. Shengyuan, P. Shengjie, N.K. Elumalai, S. Ramakrishna, Rice grain-shaped TiO2?CNT composite—a functional material with a novel morphology for dye-sensitized solar cells, J. Photochem. Photo Biol. A: Chem. 231 (2012) 9–18.
[11] F. Petronella, M.L. Curri, M. Striccoli, E. Fania, C. Mateo-Mateo, R.A. Alvarez-Puebla, T. Sibillano, C. Giannini, M.A. Correa-Duarte, R. Comparelli, Direct growth of shape controlled TiO2 nanocrystals onto SWCNTs for highly active photocatalytic materials in the visible, Appl. Cat. B: Environ. 178 (2015) 91–99.
[12] X. Liu, R. Yan, J. Zhu, X. Huo, X. Wang, Development of a photoelectrochemical lactic dehydrogenase biosensor using multi-wall carbon nanotube-TIO2 nanoparticle composite as coenzym regenaration tool, Electrochim. Acta 173 (2015) 260–267.
[13] Y. Xie, S.H. Heo, S.H. Yoo, G. Ali, S.O. Cho, Synthesis and photocatalytic activity of anatase TiO_2 nanoparticles-coated carbon nanotubes, Nanoscale Res. Lett. 5 (2010) 603–607.
[14] D.J. Cooke, D. Eder, J.A. Elliott, Role of benzyl alcohol in controlling the growth of TiO2 on carbon nanotubes, J. Phys. Chem. C 114 (2010) 2462–2470.
[15] M.D. Archer, A.J. Nozik, Nanostructured and photoelectrochemical systems for solar photon conversion, World Sci. (2008) 284–285.
[16] U.O. Akkaya Arıer, F.Z. Tepehan, Controlling the particle size of nanobrookite TiO2 thin films, J. Alloys Comp. 509 (2011) 8262–8267.
[17] U.O. Akkaya Arıer, F.Z. Tepehan, Influence of heat treatment on the particle size of nanobrookite TiO2 thin films produced by sol–gel method, Surf. Coat. Technol. 206 (2011) 37–42.
[18] L.E. Brus, Electron–electron and electron-hole interactions in small semiconductor crystallites: the size dependence of the lowest excited electronic state, J. Chem. Phys 80 (1984) 4403–4409.
[19] N. Satoh, K. Yamamoto, Quantum size titanium oxide templated with a (-conjugated dendrimer: crystal structure in the quantum size domain, Synth. Metal 159 (2009) 813–816.
[20] H. Lin, et al., Size dependency of nanocrystalline TiO2 on its optical property and photocatalytic reactivity exemplified by 2-chlorophenol, Appl. Catal. B: Environ. 68 (2006) 1–11.